The International Journal of Biochemistry & Cell Biology 62 (2015) 132–141

Contents lists available at ScienceDirect

The International Journal of Biochemistry & Cell Biology

journal homepage: www.elsevier.com/locate/biocel

Phosphatidylinositol-3-kinase as a putative target for anticancer action of clotrimazole

Cristiane M. Furtado[a,b,1], Mariah C. Marcondes[a,1], Renato S. Carvalho[a], Mauro Sola-Penna[c], Patricia Zancan[a,*]

[a] Laboratório de Oncobiologia Molecular (LabOMol), Departamento de Biotecnologia Farmacêutica (BioTecFar), Faculdade de Farmácia, Centro de Ciencias da Saúde, Universidade Federal do Rio de Janeiro, Rio de Janeiro, Brazil
[b] Programa de Pós-graduação em Bioquímica, Instituto de Química, Universidade Federal do Rio de Janeiro, Rio de Janeiro, Brazil
[c] Laboratório de Enzimologia e Controle do Metabolismo (LabECoM), Departamento de Biotecnologia Farmacêutica (BioTecFar), Faculdade de Farmácia, Centro de Ciencias da Saúde, Universidade Federal do Rio de Janeiro, Rio de Janeiro, Brazil

ARTICLE INFO

Article history:
Received 16 August 2014
Received in revised form 8 February 2015
Accepted 9 March 2015
Available online 17 March 2015

Keywords:
Anticancer drugs
Metabolism
Growth signal
Autophagy
Apoptosis

ABSTRACT

Clotrimazole (CTZ) has been proposed as an antitumoral agent because of its properties that inhibit glycolytic enzymes and detach them from the cytoskeleton. However, the broad effects of the drug, e.g., acting on different enzymes and pathways, indicate that CTZ might also affect several signaling pathways. In this study, we show that CTZ interferes with the human breast cancer cell line MCF-7 after a short incubation period (4 h), thereby diminishing cell viability, promoting apoptosis, depolarizing mitochondria, inhibiting key glycolytic regulatory enzymes, decreasing the intracellular ATP content, and permeating plasma membranes. CTZ treatment also interferes with autophagy. Moreover, when the incubation is performed under hypoxic conditions, certain effects of CTZ are enhanced, such as phosphatidylinositol-3-phosphate kinase (PI3K), which is inhibited upon CTZ treatment; this inhibition is potentiated under hypoxia. CTZ-induced PI3K inhibition is not caused by upstream effects of CTZ because the drug does not affect the interaction of the PI3K regulatory subunit and the insulin receptor substrate (IRS)-1. Additionally, CTZ directly inhibits human purified PI3K in a dose-dependent and reversible manner. Pharmacologic and in silico results suggest that CTZ may bind to the PI3K catalytic site. Therefore, we conclude that PI3K is a novel, putative target for the antitumoral effects of CTZ, interfering with autophagy, apoptosis, cell division and viability.

© 2015 Elsevier Ltd. All rights reserved.

1. Introduction

Cancer cells are characterized by a unique energetic metabolic profile, conducting constant, highly activated fermentative glycolysis, even with a normal oxygen supply (Yeung et al., 2008; Zheng, 2012). Simultaneously, these cells catabolize glutamine, used not only to generate a redox potential but also as a major carbon source (Zu and Guppy, 2004). This entire phenomenon is known as the *Warburg effect* because it was first described by Otto Warburg more than 50 years ago (Bayley and Devilee, 2012). Currently, most of these metabolic alterations are a consequence of the stable activation of hypoxia induced factor 1 (HIF-1), even in the presence of oxygen (Yeung et al., 2008). Additionally, it is well accepted that aerobic, fermentative glycolysis is the major energy furnisher to these cells, whereas glutamine is mainly used to generate substrates to biosynthesize amino acids, lipids and carbohydrates (Zu and Guppy, 2004). Thus, many studies have aimed at interfering with this altered metabolism and, therefore, with cancer viability (Parks et al., 2013).

Although the *Warburg effect* does not depend on the oxygen supply, it is known that cancer cell metabolism changes during hypoxic conditions (Parks et al., 2013), which most likely occurs because cancer cells are even more dependent on fermentative glycolysis as a source of energy under hypoxia (Semenza, 2008). In this context, HIF-1 is a key participant, triggering the intracellular effects of hypoxia (Semenza, 2013). Therefore, HIF-1 has been proposed as a target to interfere with cancer metabolism and control proliferation (Semenza, 2003). However, HIF-1 interferences occur at the expression level, making both the interference and the

* Corresponding author at: Laboratório de Oncobiologia Molecular (LabOMol), Departamento de Biotecnologia Farmacêutica (BioTecFar), Faculdade de Farmácia, Centro de Ciencias da Saúde, Universidade Federal do Rio de Janeiro, Av. Carlos Chagas Filho 373, CCS, Bloco Bss Sala 19, Ilha do Fundão, 21941-902 Rio de Janeiro, RJ, Brazil. Tel.: +55 21 2560 8438; fax: +55 21 2260 9192x203.
E-mail address: pzancan@ufrj.br (P. Zancan).
[1] Both authors contributed equally to this work.

http://dx.doi.org/10.1016/j.biocel.2015.03.004
1357-2725/© 2015 Elsevier Ltd. All rights reserved.

consequences difficult to control (Semenza, 2013). Furthermore, the side effects, mainly to non-tumor cells, would be extensive. Thus, some authors have proposed direct interference with the glycolytic pathway as a way to attack cancer cells with minor effects to non-cancer cells (Parks et al., 2013; Zheng, 2012). This approach is viable because most non-cancer cells are not strictly dependent on glycolysis as an energy source (Parks et al., 2013; Semenza, 2008; Zheng, 2012).

Clotrimazole (CTZ) is an imidazole derivative that presents antiproliferative properties (Khalid et al., 2005; Penso and Beitner, 2002a). We have demonstrated that this drug directly interferes with glycolytic enzymes, thus inhibiting glycolysis (Coelho et al., 2011; Furtado et al., 2012; Marcondes et al., 2010; Meira et al., 2005; Zancan et al., 2007). The deleterious effects of CTZ are more pronounced in aggressive, metastatic cancer cells than in non-metastatic cancer cells and are minimal to non-tumor cells (Coelho et al., 2011; Furtado et al., 2012). However, the overall effect of CTZ cannot be explained only via glycolytic enzyme inhibition because it is devastating to cell shape, migration and invasiveness. Moreover, the drug rapidly damages cancer cell plasma membranes. These broad effects suggest that CTZ is most likely interfering with signaling pathways that control cell glycolytic metabolism, physiology and morphology. A simple guess suggests the participation of the insulin/growth factors pathway. This pathway can be grossly divided into two branches: the metabolic branch, in which phosphatidylinositol-3-kinase (PI3K) plays a key role, and the anabolic branch, in which mitogen-activated protein kinase (MAPK) plays a key role (Hashimoto et al., 2014).

To investigate other targets for CTZ antitumoral properties, we evaluated the effects of the drug on the metabolism and physiology of the human breast cancer cell line MCF-7. The results presented in this report reveal targets for CTZ effects on cancer cells.

2. Materials and methods

2.1. Materials

Clotrimazole, NAD^+, NADH, $NADP^+$, ATP, ADP, fructose 6-phosphate, lactate, glucose 6-phosphate, phosphoenolpyruvate, hexokinase, lactate dehydrogenase, aldolase, glucose 6-phosphate dehydrogenase, triosephosphate isomerase, and α-glycerophosphate were purchased from Sigma Chemical, St. Louis, MO, USA. Other reagents were of the highest purity available.

2.2. Cell and culture conditions

The human breast cancer cell line MCF-7 was obtained from the Cell Bank of Hospital Universitário Clementino Fraga Filho, UFRJ, Brazil, and Prof. Dr. Mitzi Brentani from the University of São Paulo, USP, Brazil, and was maintained in DMEM (Dulbecco's modified Eagle's medium; Invitrogen, São Paulo, SP, Brazil) supplemented with 10% (v/v) FBS (fetal bovine serum; Invitrogen) and L-glutamine (Zancan et al., 2010). The cells were grown for 4 h at 37 °C in a 5% CO_2 atmosphere or maintained in a hypoxia chamber MIC101 (Hypoxia Incubator Chamber; StemCell Technologies, Vancouver, BC, Canada). The considered hypoxic condition had a gas mixture of 5% O_2 and 94% N_2 and was obtained from White Martins Praxair Inc. (Osasco, SP, Brazil). The sample was kept in an oven at 37 °C.

2.3. MTT assay

The MCF-7 cell mitochondrial reductive activity was assayed using the MTT assay as described previously (Spitz et al., 2009). Cells were seeded in 96-well plates (5×10^4 cells/well) and grown to confluence. Then, the medium was removed, fresh medium was added, and the cells were returned to the incubator in the presence of different concentrations of clotrimazole (0–50 μM). After 24 h, the cells were incubated with 5 mg/mL MTT reagent (3,4,5-dimethiazol-2,5-diphenyltetrazolium bromide, Sigma–Aldrich Co., St. Louis, MO, USA) for 3 h. Thereafter, the formazan crystals were dissolved in DMSO, and the absorbance at 560 nm was evaluated using a VICTOR3 multilabel microplate reader (PerkinElmer, Waltham, MA, USA) with subtraction of the background absorbance at 670 nm (Spitz et al., 2009).

2.4. ATP quantitative measurement

Cells were seeded in 96-well plates (5×10^4 cells/well) and grown to confluence. Then, the medium was removed, fresh medium was added, and the cells were treated with different concentrations of clotrimazole (0–50 μM) for 24 h. After this incubation, the medium was removed, and the ATP Lite kit reagents (Luminescence ATP Detection Assay System – PerkinElmer, Waltham, MA, USA) were added. This system is based on the production of light by luciferase because it consumes ATP and D-luciferin. The luminescence is proportional to the concentration of cellular ATP and was analyzed using a VICTOR3 multilabel microplate reader (PerkinElmer, Waltham, MA, USA) (Furtado et al., 2012).

2.5. Leaked LDH activity

Cells were seeded in 96-well plates (5×10^4 cells/well) and grown to confluence. Then, the medium was removed, fresh medium was added, and the cells were returned to the incubator and treated for 4 h under normoxia or hypoxia in the presence of the compounds indicated in the abscissa. Then, the medium was removed, and the amount of leaked lactate dehydrogenase (LDH) was evaluated by monitoring the reduction of NAD^+ to NADH via the absorbance at 340 nm using a VICTOR3 multilabel microplate reader (PerkinElmer, Waltham, MA, USA) (Furtado et al., 2012).

2.6. Measurement of hexokinase, phosphofructokinase, pyruvate kinase and glucose 6-phosphate dehydrogenase activities

Cells were seeded in 24-well plates (2×10^5 cells/well) and grown to confluence. Then, the medium was removed, fresh medium was added, and the cells were treated with or without 50 μM clotrimazole for 24 h. After this incubation, the cells were trypsinized, centrifuged (10 min × 1000 × *g*), resuspended in 10 mM potassium phosphate buffer (pH 7.4), and counted using a hemacytometer. All protein concentrations were analyzed following Lowry et al. (1951).

The phosphofructokinase (PFK) activity was measured using an enzyme-coupled method in a reaction buffer containing 5 mM $MgCl_2$, 1 mM fructose 6-phosphate, 1 mM ATP, 0.2 mM NADH, 2 U/ml aldolase, 4 U/ml triosephosphate isomerase and 2 U/ml α-glycerophosphate dehydrogenase in 50 mM Tris–HCl (pH 7.4). The reaction was monitored spectrophotometrically by the absorbance at 340 nm associated with the oxidation of NADH to NAD^+ in a VICTOR3 multilabel microplate reader (PerkinElmer, Waltham, MA, USA) (Real-Hohn et al., 2010).

The hexokinase (HK) activity was assessed in a basic medium containing 50 mM Tris–HCl (pH 7.4), 5 mM $MgCl_2$, 1 mM glucose, 1 mM ATP, 0.2 mM NAD^+ and 1 U/ml glucose 6-phosphate dehydrogenase. The reaction was monitored spectrophotometrically via the loss of absorbance at 340 nm associated with the reduction of NAD^+ to NADH in a VICTOR3 multilabel microplate reader (PerkinElmer, Waltham, MA, USA) (Leite et al., 2011).

The pyruvate kinase (PK) activity was measured in a medium containing 50 mM Tris–HCl (pH 7.4), 5 mM $MgCl_2$, 120 mM KCl,

1 mM phosphoenolpyruvate, 1 mM ADP, 0.2 mM NADH and 20 U/ml lactate dehydrogenase. The reaction was monitored spectrophotometrically by the absorbance at 340 nm associated with the oxidation of NADH to NAD^+ in a VICTOR3 multilabel microplate reader (PerkinElmer, Waltham, MA, USA) (Leite et al., 2011).

The glucose-6-phosphate dehydrogenase (G6PDH) activity was assayed in a medium containing 50 mM Tris–HCl (pH 7.4), 5 mM $MgCl_2$, 0.5 mM glucose 6-phosphate and 0.2 mM $NADP^+$. The reaction was monitored spectrophotometrically at 340 nm in a VICTOR3 multilabel microplate reader (PerkinElmer, Waltham, MA, USA) to identify the reduction of $NADP^+$ to NADPH (Furtado et al., 2012).

All reactions were initiated via the addition of an aliquot of cellular homogenate. Experiments lacking the coupled enzymes were performed to control for non-specific oxidation/reduction.

2.7. Evaluation of live/dead assay, cell cycle assay, apoptosis activation, BCL-2 activation, mitochondrial polarization, autophagy induction, PI3K activation and MAPK activation

All of these parameters were evaluated using a Muse® Cell Analyzer (Merck Millipore, Billerica, MA, USA) and the appropriate reagent kit. The kits used were Muse® Count & Viability Assay Kit, Muse® Cell Cycle Assay Kit, Muse® Annexin V & Dead Cell Assay Kit, Muse® Bcl-2 Activation Dual Detection Assay Kit, Muse® Mitopotential Assay Kit, Muse® Autophagy LC3-Antibody Based Kit, Muse® PI3K Activation Dual Detection Assay Kit and Muse® MAPK Activation Dual Detection Assay Kit. For autophagy induction, cells were incubated under normoxia or hypoxia in DMEM medium supplemented with 10% FBS (control) or without FBS (starvation). After 4 h of treatment, cells were evaluated following the kit manufacturers' protocols.

2.8. Western blots

MCF7 cells were plated in 96-well plates (5×10^3 cells/well), allowed to attach for 24 h and treated with 50 μM CTZ or 1 μM Wortmannin for 1.5 h. Cells were lysed and were either submitted to immunoprecipitation in the presence of an anti-insulin receptor substrate (IRS)-1 antibody (Cell Signaling, 2382, used in the dilution of 1:100) or were directly submitted to SDS-PAGE for further immunobloting against anti-IRS-1 (Cell Signaling, 2382, used in the dilution of 1:1000), anti-phospho(S1101)-IRS-1 (Cell Signaling, 2385, used in the dilution of 1:500), anti-S6K (Cell Signaling, 2903, used in the dilution of 1:1000), anti-phospho-S6K (Cell Signaling, 9234, used in the dilution of 1:500), anti-PTEN (Santa Cruz Biotechnology, sc-7974, used in the dilution of 1:1000) or anti-phospho-PTEN (Santa Cruz Biotechnology, sc-377573, used in the dilution of 1:1000). The immunoprecipitation product was further submitted to SDS-PAGE and immunoblotting against IRS-1 and p85. As loading controls, the membranes were immunoblotted against anti-β-actin (Cell Signaling, 4967, used in the dilution of 1:10,000). All procedures were performed according to Tremblay and Marette (2001).

2.9. Clotrimazole/Ly294002 combination viability assay

MCF7 cells were plated in 96-well plates (5×10^3 cells/well), allowed to attach for 24 h and treated with different concentrations of: (a) CTZ (0, 6.25, 12.5, 25 and 50 μM), (b) Ly294002 (0, 12.5, 25, 50 and 100 μM), or (c) the combined drugs following a 4×4 matrix of the used concentrations. Cells were treated for 48 h and their viability was assessed using an MTT assay, as previously described (Mosmann, 1983).

2.10. PI3K activity evaluation

PI3K activity was evaluated using an ELISA kit and human purified PI3K alpha (Echelon Biosciences Inc., Salt Lake City, UT, USA).

2.11. Molecular docking

Molecular docking was performed using the free online platform Mcule (https://mcule.com) as described previously (Tam et al., 2012). The human PI3K, subunit gamma (PDB accession number 2A4Z), was use to dock CTZ, LY294002 and ATP.

2.12. Statistical analysis

Graphs, statistical analyses and non-linear regressions were prepared using the software Prism 6 for Mac OS X (GraphPad Software Inc., La Jolla, CA, USA). All values were shown as the means ± standard error of the mean (S.E.M.). Two-tailed ANOVA and Bonferroni's post hoc test were used to compare differences among the experimental data. P values ≤ 0.05 were accepted as statistically significant.

3. Results

3.1. CTZ decreases MCF-7 cell viability arresting the cells at G0/G1 phase

Aimed at testing whether CTZ would be more deleterious to MCF-7 cells under hypoxia than under normoxia, a cell viability assay was performed (Fig. 1A). This experiment reveals that, under normoxic conditions, MCF-7 cell viability decreases from 98 ± 2% in the control to 77 ± 5% after incubation in the presence of 50 μM CTZ for 4 h ($P < 0.05$, two-tailed ANOVA, Bonferroni's post hoc test). The anti-cancer drug paclitaxel also decreases MCF-7 cell viability to 86 ± 5% ($P < 0.05$, two-tailed ANOVA, Bonferroni's post hoc test). Under hypoxia, the control cell viability is 96 ± 3%, and it decreases to 61 ± 5% and 83 ± 7% after incubation for 4 h with 50 μM CTZ and 2 μM paclitaxel, respectively ($P < 0.05$, two-tailed ANOVA, Bonferroni's post hoc test). Comparing the results under hypoxia and normoxia, it can be observed that CTZ is more deleterious in hypoxia than normoxia ($P < 0.05$, two-tailed ANOVA, Bonferroni's post hoc test). The enhanced effects of CTZ under hypoxia are also observed by evaluating the cell cycle phase (Fig. 1B and C). Under normoxia, CTZ does not promote any significant change in the MCF-7 cell cycle phase, although paclitaxel arrest cells at the G2/M phase (Fig. 1B). However, under hypoxia, CTZ arrests the cells at the G0/G1 phase (Fig. 1C). Note that the arrest promoted by paclitaxel at the G2/M phase under both normoxia and hypoxia is accompanied by a decrease of cells in the G0/G1 phase. Conversely, the arrest promoted by CTZ at the G0/G1 phase includes a cell decrease in the G2/M phase. The S phase is not affected by any of the drugs. Regardless of the phase in which cells are arrested, these phenomena indicate that these drugs negatively affect cell proliferation.

3.2. CTZ induces apoptosis, necrosis and depolarizes mitochondria in MCF-7 cells

To determine whether CTZ is also promoting cell death, we assessed apoptotic and necrotic cells after CTZ treatment under normoxia and hypoxia. As a positive control, we used 1 μM staurosporin, a well-known apoptosis inductor. Under normoxic conditions, incubation of MCF-7 cells with 50 μM CTZ or 1 μM staurosporin promotes a decrease in live cells with a parallel increase in apoptotic and necrotic cells (Fig. 2A). For both drugs, induction of apoptosis is more significant than necrosis. Moreover, staurosporin is more efficient than CTZ at diminishing the number of

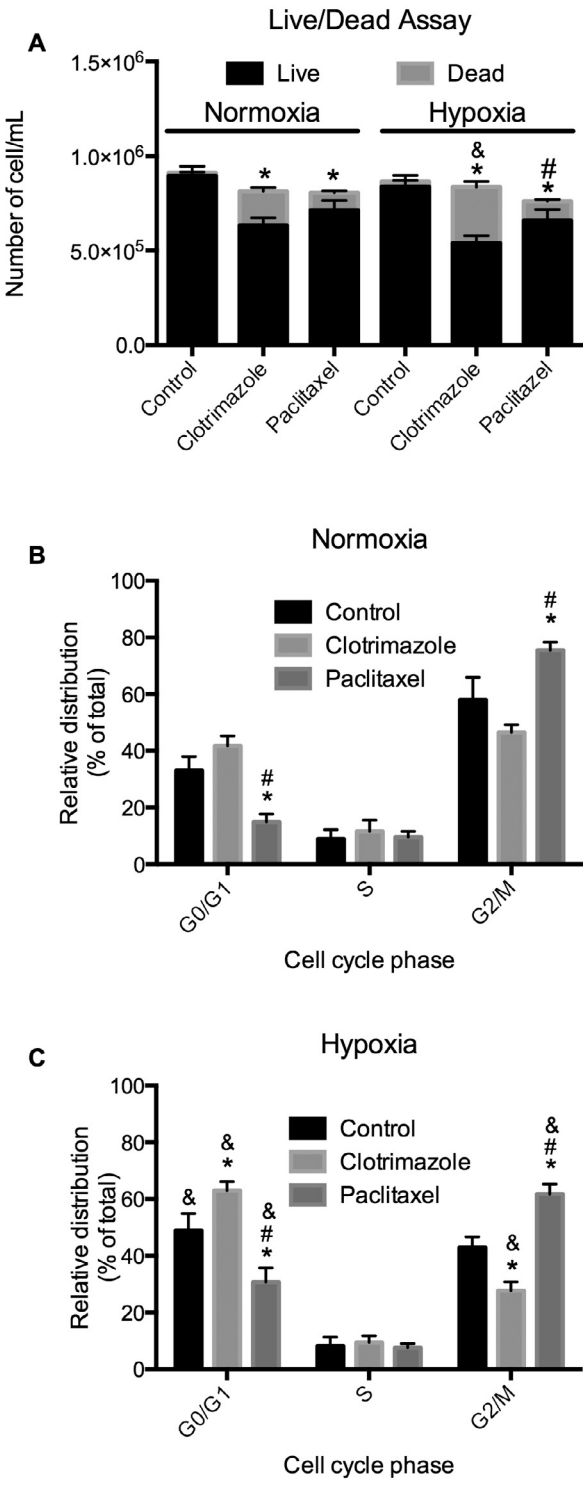

Fig. 1. CTZ interferes with the cell cycle and cell survival. Cells were grown and treated as described in the Material and Methods section in the absence or presence of 50 μM CTZ or 2 μM paclitaxel. Panel (A): live and dead assay evaluated after 4 h of treatment during normoxia or hypoxia. Panel (B): cell cycle phases evaluated after 4 h of treatment during normoxia. Panel (C): cell cycle phases evaluated after 4 h of treatment during hypoxia. Data are shown as the mean ± standard error of at least three independent experiments performed at least in duplicate ($n = 3$). $^{*}P < 0.05$ compared to the control in the same group. $^{\#}P < 0.05$ compared to CTZ in the same group. $^{\&}P < 0.05$ compared to normoxia under the same conditions. All statistics were performed by two-tailed ANOVA using Bonferroni's post hoc test.

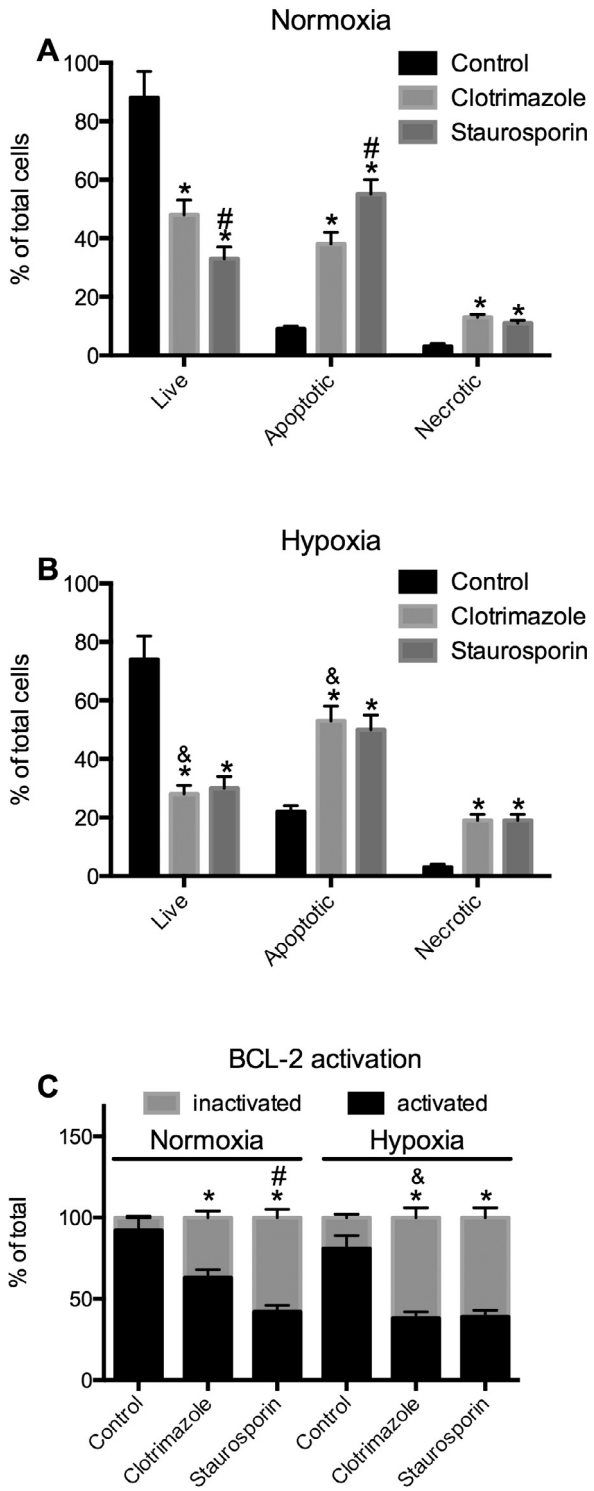

Fig. 2. CTZ induces apoptosis and inactivation of BCL-2. Cells were grown and treated as described in Section 2 in the absence or presence of 50 μM CTZ or 1 μM staurosporin. Panel (A): apoptosis and necrosis assay evaluated after 4 h of treatment during normoxia. Panel (B): apoptosis and necrosis assay evaluated after 4 h of treatment during hypoxia. Panel (C): BCL-2 activation evaluated after 4 h of treatment during normoxia or hypoxia. Data are shown as the mean ± standard error of at least three independent experiments performed at least in duplicate ($n = 3$). $^{*}P < 0.05$ compared to control in the same group. $^{\#}P < 0.05$ compared to CTZ in the same group. $^{\&}P < 0.05$ compared to normoxia under the same condition. All statistics were performed by two-tailed ANOVA using Bonferroni's post hoc test.

live cells and promoting apoptosis (Fig. 2A). However, the efficiency of CTZ increases under hypoxia, decreasing the number of live cells and promoting apoptosis, compared to normoxic conditions (Fig. 2B). Under hypoxia, there is no significant difference between the effects of CTZ and staurosporin on these mechanisms of cell death. Moreover, the anti-apoptotic regulatory protein, BCL-2, was evaluated. The activated (phosphorylated) levels of BCL-2 diminish upon CTZ and staurosporin treatment, under normoxia and hypoxia (Fig. 2C). However, staurosporin is more effective than CTZ under normoxia, but under hypoxia, CTZ increases its effectiveness, becoming as efficient as staurosporin (Fig. 2C).

To better understand the mechanisms involved in CTZ-induced cell death, we evaluated the mitochondrial potential of treated cells. Staurosporin was used as a positive control. This assay differentiates among cells of average size and polarized mitochondria (live), average size and depolarized mitochondria (depolarized), and reduced cell size and depolarized mitochondria (dead). Under normoxia, both CTZ and staurosporin decrease the number live cells, increasing the depolarized and dead cell counts to similar levels, compared to the control (Fig. 3A). Hypoxia slightly reduces the polarization of mitochondria, decreasing the live group while increasing the depolarized and dead group, compared to normoxic conditions (Fig. 3B). These effects are enhanced upon treatment with CTZ or staurosporin. However, under hypoxia, CTZ is more efficient at depolarizing mitochondria than staurosporin (Fig. 3B).

3.3. CTZ decreases MCF-7 cells autophagy through direct inhibition of PI3K

Autophagy is an important mechanism of cell survival, especially when nutrient availability is limited. We assessed the effects of CTZ on autophagy induction in MCF-7 cells subjected to starvation under normoxia and hypoxia. Resveratrol and Wortmannin were used as positive and negative controls, respectively. In normoxic conditions, CTZ decreases the induction of autophagy in $18 \pm 1\%$ for the control and $68 \pm 6\%$ for those under starvation (Fig. 4A, $P < 0.05$, two-tailed ANOVA, Bonferroni's post hoc test). Hypoxia increased the induction of autophagy 4–5 times in the control, with minor effects during starvation (Fig. 4B). However, the effects of CTZ on autophagy induction are greatly increased during hypoxia, whereas CTZ reduces the induction of autophagy by $88 \pm 5\%$ in the control and $94 \pm 6\%$ for those under starvation (Fig. 4B). The activation of autophagy by resveratrol also increased during hypoxia, whereas the inhibition by Wortmannin remains unaltered (Fig. 4A and B). This effect can be explained by evaluating PI3K activation. Hypoxia activates PI3K at 50% (Fig. 4C). However, this effect is opposite in the presence of CTZ. The drug promotes a 15% decrease in PI3K activation during normoxia and a 70% decrease during hypoxia, compared to the control (Fig. 4C, $P < 0.05$, two-tailed ANOVA, Bonferroni's post hoc test). Additionally, in the presence of CTZ, hypoxia decreases PI3K activation by 40% (Fig. 4C, $P < 0.05$, two-tailed ANOVA, Bonferroni's post hoc test). The classic PI3K inhibitor Wortmannin also decreases PI3K activation during normoxia and hypoxia (Fig. 4C, $P < 0.05$, two-tailed ANOVA, Bonferroni's post hoc test), but the PI3K activation is not different during normoxia and hypoxia. We have also evaluated the effects of CTZ on MAPK activation (Fig. 4D). Although CTZ slightly inhibits MAPK, the efficiency is not comparable to the MEK inhibitor PD98059, and the effects are not different when comparing normoxic and hypoxic conditions (Fig. 4D).

To further explore PI3K inhibition by CTZ, we evaluated the effects of the drug up- and downstream PI3K signaling. For the upstream event, we analyzed the association of the p85 subunit of PI3K to IRS-1 in response to insulin stimulation. The presence of 1 μM Wortmannin or 50 μM CTZ slightly increases insulin-stimulated association between p85 and IRS-1 (Fig. 4E). This result reveals that CTZ-induced PI3K inhibition is not caused by upstream activation of the enzyme. However, phosphorylation of S6K, a downstream event of PI3K signaling, is abolished by the presence of 50 μM CTZ or the classic PI3K inhibitor Wortmannin (Fig. 4F). This lack of downstream PI3K signaling cannot be attributed to an increased degradation of PIP_3 because CTZ treatment, as well as Wortmannin, does not affect PTEN phosphorylation, which would in turn promote PIP_3 degradation (Fig. 4F). Remaining downstream in PI3K signaling pathway, both CTZ and Wortmannin, promote a reduction in the levels of IRS-1 phosphorylation in serine 1101, which is promoted by either S6K or PKC (Fig. 4G). Furthermore, the effects of CTZ are not additive to the reversible PI3K inhibitor, LY294002. This PI3K inhibitor promoted a dose-dependent decrease on MCF-7 cell viability, an effect that is not augmented by CTZ (Fig. 4H and I). Indeed, in the presence of 25 or 50 μM CTZ, which, respectively decrease MCF-7 cell viability to $60 \pm 5\%$ and $51 \pm 4\%$, LY294002 does not further affect cell viability up to 100 μM (Fig. 4I). CTZ was also able to inhibit PI3K activity in a direct assay using a purified enzyme (Fig. 4J). As with Wortmannin and LY294002, CTZ inhibited the enzyme in a dose-dependent manner, presenting an IC_{50} of 7.3 ± 0.8 μM, as calculated by non-linear regression. The calculated IC_{50} for Wortmannin and LY294002 are 3.7 ± 0.5 nM and 0.52 ± 0.05 μM, respectively. In the simultaneous presence of CTZ (10 μM) and LY294002 (0.5 μM), no additive effect on PI3K inhibition is observed (Fig. 4K), confirming the results presented in Fig. 4H and I. The reversibility of CTZ-induced PI3K

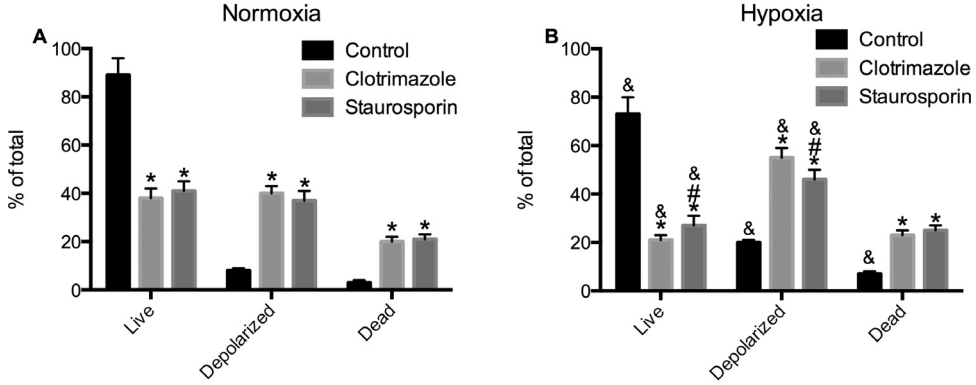

Fig. 3. CTZ promotes mitochondria depolarization. Cells were grown and treated as described in Section 2 in the absence or presence of 50 μM CTZ or 1 μM staurosporin. Panel (A): mitochondria polarization assay evaluated after 4 h of treatment during normoxia. Panel (B): mitochondria polarization assay evaluated after 4 h of treatment during hypoxia. Data are shown as the mean ± standard error of at least three independent experiments performed at least in duplicate ($n = 3$). $^{*}P < 0.05$ compared to control in the same group. $^{\#}P < 0.05$ compared to CTZ in the same group. $^{\&}P < 0.05$ compared to normoxia under the same condition. All statistics were performed by two-tailed ANOVA using Bonferroni's post hoc test.

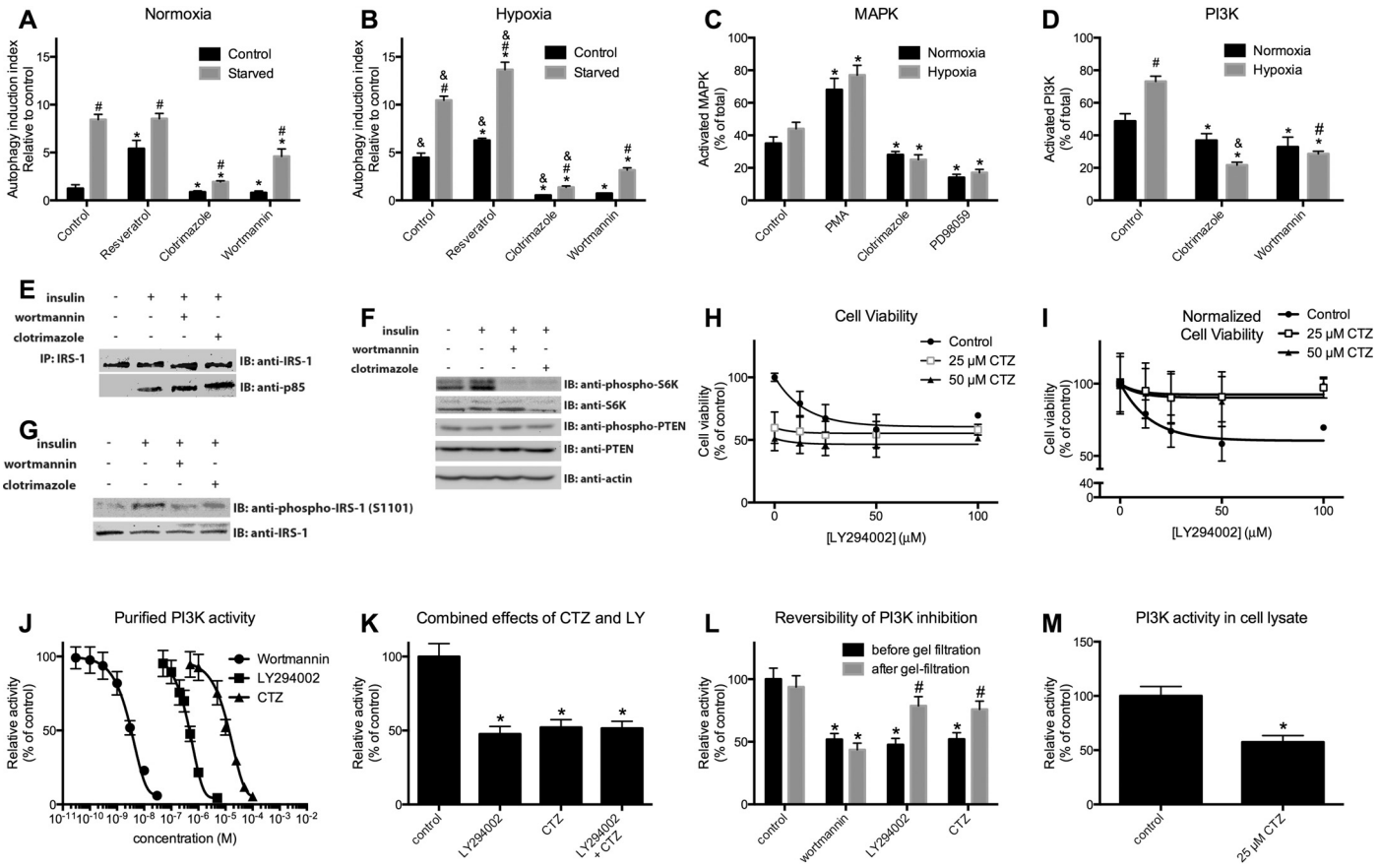

Fig. 4. CTZ inhibits autophagy, MAPK and PI3K. Cells were grown and treated as described in Section 2 in the absence or presence of 50 μM CTZ, 50 μM resveratrol, 1 μM Wortmannin or 1 μM PD98059. Panel (A): autophagy induction assay evaluated after 4 h treatment during normoxia. Panel (B): autophagy induction assay evaluated after 4 h of treatment during hypoxia. Panel (C): MAPK activation assay evaluated after 4 h of treatment during normoxia or hypoxia. Panel (D): PI3K activation assay evaluated after 4 h of treatment during normoxia or hypoxia. Panel (E): evaluation of the interaction between p85 and IRS-1 through immunoprecipitation of IRS-1 and immunoblotting against IRS-1 and p85. Panel (F): evaluation of events downstream PI3K signaling through immunoblotting against S6K and phospho-S6K and PTEN and phospho-PTEN. Panel (G): evaluation of phosphorylation on serine 1101 of IRS-1. Panel (H): effects of LY294002 on MCF-7 viability in the absence and presence of CTZ. Panel (I): re-plot of panel (H) normalized to the absence of LY294002. Panel (J): dose–response curve of PI3K inhibition by Wortmannin, LY294002 and CTZ. Panel (K): effects of LY294002 (0.5 μM), CTZ (10 μM) and both combined (0.5 μM and 10 μM for LY294002 and CTZ, respectively). Panel (L): reversibility of the effects of Wortmannin (3 nM), LY294002 (0.5 μM) and CTZ (1 μM). Panel (M): PI3K activity evaluated in whole-cell lysate in the absence (control) and the presence of 25 μM CTZ. Graphical data are shown as the mean ± standard error of, at least, three independent experiments performed, at least, in duplicate ($n = 3$). $^{*}P < 0.05$ compared to control in the same group. $^{\#}P < 0.05$ compared to CTZ in the same group. $^{\&}P < 0.05$ compared to normoxia under the same condition. For panel (L), $^{\#}P < 0.05$ compared to before gel-filtration. All statistics were performed by two-tailed ANOVA, using Bonferroni's post hoc test.

inhibition was evaluated by incubating the purified enzyme in the presence of 10 μM CTZ for 10 min followed by removal of the drug using a desalting column (PD SpinTrap G25, GE Life Sciences, Buckinghamshire, UK) and then measuring PI3K activity. Wortmannin (3 nM) and LY294002 (0.5 μM) were used as irreversible and reversible controls, respectively. This experiment reveals that, as with LY294002, CTZ-induced PI3K inhibition is reversible (Fig. 4L). To confirm PI3K inhibition in the presence of other cellular components, PI3K activity was evaluated in a whole MCF-7 lysate in the absence and the presence of 25 μM CTZ, where the drug also inhibited the enzyme (Fig. 4M).

3.4. CTZ decreases energy metabolism in MCF-7 cells

Finally, the effects of CTZ on the regulatory glycolytic enzymes, G6PDH, intracellular ATP content, mitochondrial reductive activity and plasma membrane integrity were evaluated during normoxia and hypoxia. All of the inhibitors used as negative and positive controls (except PMA) were used in these experiments. With regard to the regulatory glycolytic enzymes, HK, PFK and PK, hypoxia only affects the former; that is, 20% activation compared to normoxia (Fig. 5A, $P < 0.05$, two-tailed ANOVA, Bonferroni's post hoc test). As expected and previously published, CTZ inhibits all of them, although this inhibitory effect is not different between normoxia and hypoxia (Fig. 5A–C for HK, PFK and PK, respectively). Among the other drugs used, differences between normoxia and hypoxia are observed for Wortmannin, which is less efficient at inhibiting HK and PFK during hypoxia (this enzyme is not inhibited by Wortmannin under hypoxia), and more efficient at inhibiting PK during hypoxia (Fig. 5A–C for HK, PFK and PK, respectively; $P < 0.05$, two-tailed ANOVA, Bonferroni's post hoc test). For this latter enzyme, resveratrol and paclitaxel also showed different effects under normoxia and hypoxia, whereas resveratrol does not inhibit the enzyme under hypoxia and paclitaxel is more efficient at inhibiting PK under hypoxia than normoxia (Fig. 5C, $P < 0.05$, two-tailed ANOVA, Bonferroni's post hoc test). G6PDH is also inhibited by CTZ, but no difference is observed between normoxia and hypoxia (Fig. 5D). This enzyme is not inhibited by paclitaxel or Wortmannin, whereas inhibition by staurosporin and resveratrol are less efficient during hypoxia than normoxia (Fig. 5D, $P < 0.05$, two-tailed ANOVA, Bonferroni's post hoc test).

Intracellular ATP content is directly diminished by hypoxia, an effect that is eliminated in the presence of resveratrol and paclitaxel (Fig. 5E, $P < 0.05$, two-tailed ANOVA, Bonferroni's post hoc test).

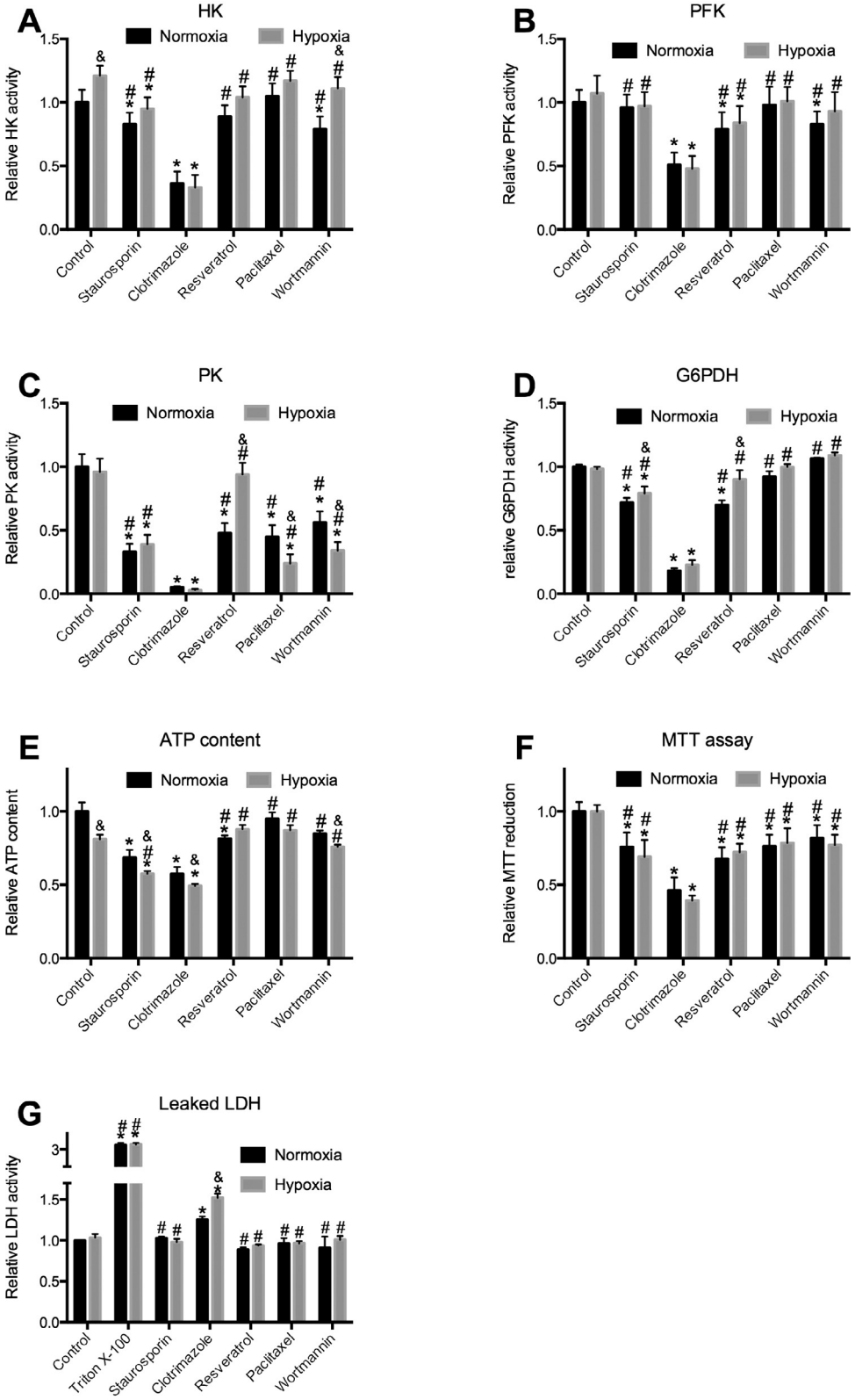

Fig. 5. CTZ inhibits glycolytic enzymes and decreases intracellular ATP content decreasing cell viability. Cells were grown and treated as described in Section 2 in the absence or presence of 50 μM CTZ, 1 μM staurosporin, 50 μM resveratrol, 1 μM Wortmannin, 2 μM paclitaxel or 0.5% triton X-100. Panel (A): HK activity evaluated after 4 h of treatment during normoxia or hypoxia. Panel (B): PFK activity evaluated after 4 h of treatment during normoxia or hypoxia. Panel (C): PK activity evaluated after 4 h of treatment during normoxia or hypoxia. Panel (D): G6PDH activity evaluated after 4 h of treatment during normoxia or hypoxia. Panel (E): intracellular ATP content evaluated after 4 h of treatment during normoxia or hypoxia. The absolute level of ATP found in control under normoxia was 17 ± 1 nmol/10^7 cells. Panel (F): MTT assay evaluated after 4 h of treatment during normoxia or hypoxia. Panel (G): leaked LDH activity evaluated after 4 h of treatment during normoxia or hypoxia. Data are shown as the mean ± standard error of at least three independent experiments performed at least in duplicate ($n = 3$). $^{*}P < 0.05$ compared to control in the same group. $^{\#}P < 0.05$ compared to CTZ in the same group. $^{\&}P < 0.05$ compared to normoxia under the same condition. All statistics were performed by two-tailed ANOVA, using Bonferroni's post hoc test.

CTZ decreases the intracellular ATP content by 40%, an effect that is potentiated under hypoxia (Fig. 5E, $P < 0.05$, two-tailed ANOVA, Bonferroni's post hoc test). Hypoxia also potentiates the effects of staurosporin and Wortmannin on the intracellular ATP content (Fig. 5E, $P < 0.05$, two-tailed ANOVA, Bonferroni's post hoc test). With regard to reductive mitochondrial activity assessed using the MTT assay, all of the compounds that were tested showed inhibitory effects, but no differences are observed between normoxic and hypoxic conditions (Fig. 5F). However, by evaluating the plasma membrane integrity, assessed by measuring the LDH activity in the cell-free culture medium at the end of the treatment, we observed that only CTZ promotes plasma membrane injury, leaking LDH to the medium (Fig. 5G). Additionally, this effect is more pronounced during hypoxia than normoxia (Fig. 5G, $P < 0.05$, two-tailed ANOVA, Bonferroni's post hoc test).

4. Discussion

We have examined some potential targets for CTZ action as an antitumoral agent. CTZ has been reported to be an anticancer agent because of it affects some glycolytic enzymes, such as HK and PFK, among others (Coelho et al., 2011; Furtado et al., 2012; Glass-Marmor and Beitner, 1997; Glass-Marmor et al., 1996; Khalid et al., 2005; Majewski et al., 2004; Marcondes et al., 2010; Meira et al., 2005; Penso and Beitner, 1998, 2002a,b; Rodríguez-Enríquez et al., 2009; Zancan et al., 2007). The drug interferes with the activities of these enzymes (Furtado et al., 2012; Marcondes et al., 2010; Zancan et al., 2007) as well as with their interactive network, including the cytoskeleton and other glycolytic enzymes (Coelho et al., 2011; Glass-Marmor and Beitner, 1997; Marcondes et al., 2010; Meira et al., 2005; Penso and Beitner, 1998, 2002a,b). As a consequence, the intracellular distribution and functionality of these enzymes are compromised, resulting in decreased cell viability. Despite that CTZ effects are not specific to a single target, it is well accepted that the drug addresses the glycolytic pathway, compromising energy production (Rodríguez-Enríquez et al., 2009). Since glycolysis is not dependent on oxygen to produce energy, it is the major energy producing pathway on a cell under hypoxia and, therefore, it is expected that CTZ should be more effective under hypoxic than under normoxic conditions. Cancer cells are adapted to hypoxic conditions as a necessity for survival in the unfavorable conditions of their microenvironments (Semenza, 2012b,c). The more adapted cancer is to hypoxia, then it is more aggressive, invasive and resistant to chemotherapy and radiation therapy (Semenza, 2012a, 2013; Wong et al., 2012). We have previously reported that CTZ is more lethal to the metastatic human breast cancer cell line MDA-mb-231 than to the non-metastatic MCF-7 cells (Furtado et al., 2012). Additionally, the effects of the drug on the non-tumoral counterpart, MCF-10A, are minimal (Furtado et al., 2012). Thus, CTZ most likely targets the adapted features of cancer cells that provide their unique metabolic profile (Hanahan and Weinberg, 2011).

Among the several adapted features of cancer cells, the dysregulated PI3K signaling pathway is a major adaptation linking cell metabolism, survival, growth, motility and morphology (Akinleye et al., 2013; Voskas et al., 2014). These PI3K properties have elected the enzyme as a target for cancer treatment drugs (Akinleye et al., 2013; Beck et al., 2014; Brana and Siu, 2012; Castillo et al., 2014). Here, we found that CTZ is an inhibitor of PI3K, an effect that is strengthened under hypoxic conditions (Fig. 4). This effect is at least partially responsible for other effects of the drug that are reported here, such as autophagy inhibition (Fig. 4), cell cycle arrest (Fig. 1), promotion of apoptosis (Fig. 2), and ATP depletion (Fig. 5). Different PI3K isoforms are involved with these different events (Castillo et al., 2014), which may indicate that the effects of CTZ on PI3K is not isoform specific. Other effects of CTZ, such as glycolytic enzyme inhibition, appears to be independent of PI3K inhibition because they are not affected as much by Wortmannin and are not different when comparing the results under normoxia and hypoxia (Fig. 5). Indeed, we have previously shown that CTZ is also able to directly inhibit PFK (Zancan et al., 2007), and because of the catalytic mechanism similarity, it would not be surprising if the inhibition of HK and PK reported were caused by a direct effect of the drug on these enzymes as well. Therefore, CTZ-induced ATP depletion might be the result of the inhibition of PI3K and its consequent inhibition of autophagy, reduction on mitochondria activity, and inhibition of glycolysis by inhibition of its major regulatory enzymes, being that the latter is not responsive to hypoxic conditions.

One possibility for the lack of a hypoxia-enhanced effect on these enzymes is that, under the evaluated conditions, the enzymes are so strongly inhibited that no difference could be observed. The data that do not support this claim show that PFK is only 50% inhibited by CTZ in the conditions tested here, which is weak enough that an enhancement would be observed. Therefore, we believe that the differences in the effects of CTZ during hypoxia and normoxia are most likely caused by the effects of the drug on a signaling pathway. Autophagy is more affected by CTZ during hypoxia than normoxia. Additionally, this pathway is dependent on PI3K activity (O Farrell et al., 2013), which in turn is also more inhibited by CTZ during hypoxia than normoxia. PI3K is normally activated by an anabolic signal, such as insulin, IGF, or others (Paplomata and O'Regan, 2014; Xu et al., 2014). All of them simultaneously trigger MAPK (Paplomata and O'Regan, 2014; Xu et al., 2014). However, the enhanced effects of CTZ on PI3K are not accompanied by enhanced effects on MAPK, suggesting that this result is not an upstream effect in the signaling pathway, which would interfere with both PI3K and MAPK branches and not only with the PIK3 branch. This hypothesis was supported because the interaction of the regulatory subunit of PI3K, p85, and its activator, tyrosine-phosphorylated IRS-1, is not negatively modulated by either CTZ or Wortmannin (Fig. 4E). Indeed, both, CTZ and Wortmannin positively regulate the interaction between p85 and IRS-1, which is most likely caused by the inhibition of PI3K and the further decrease in negatively regulatory PI3K-mediated serine-phosphorylation of IRS-1, such as has previously been demonstrated for Wortmannin, LY294002 and other PI3K inhibitors (Gual et al., 2005). We have also observed that CTZ and Wortmannin promote a decrease in the levels of S1101 phosphorylation in IRS-1 (Fig. 4G), which is the substrate for PKC (Gual et al., 2005) and S6K (Tremblay and Marette, 2001), the latter also negatively regulated by CTZ and Wortmannin (Fig. 6F).

The definitive result for PI3K inhibition by CTZ is the direct evaluation of the enzyme activity using a purified human recombinant enzyme (Fig. 4J) in which it is clear that CTZ inhibits PI3K in a dose-responsive manner, such as Wortmannin and LY294002. To further explore the mechanism of PI3K inhibition by CTZ, we performed an assay in the simultaneous presence of CTZ and LY294002. This PI3K inhibitor was used but not Wortmannin because it promotes a reversible inhibition on the enzyme, whereas the Wortmannin effects are irreversible (Walker et al., 2000). A reversible inhibitor is mandatory to evaluate synergism between drugs (Tallarida, 2001). Additionally, both Wortmannin and LY294002 bind to the identical site in PI3K, and the only difference is that Wortmannin covalently binds to a lysine residue in the catalytic site, whereas LY294002 only coordinates electrons presenting no covalent interaction (Walker et al., 2000). The effects of CTZ are not additive to the effects of LY294002 on MCF-7 cell viability because in the presence of CTZ, LY294002 presents no further effects (Fig. 4H and I). This mechanism was confirmed by direct inhibition of the enzyme in the presence of both drugs (Fig. 4K). It is notable that like LY294002, CTZ is a reversible inhibitor of PI3K (Fig. 4L). Together, these results suggest that these drugs might bind to the same site at PI3K. Therefore,

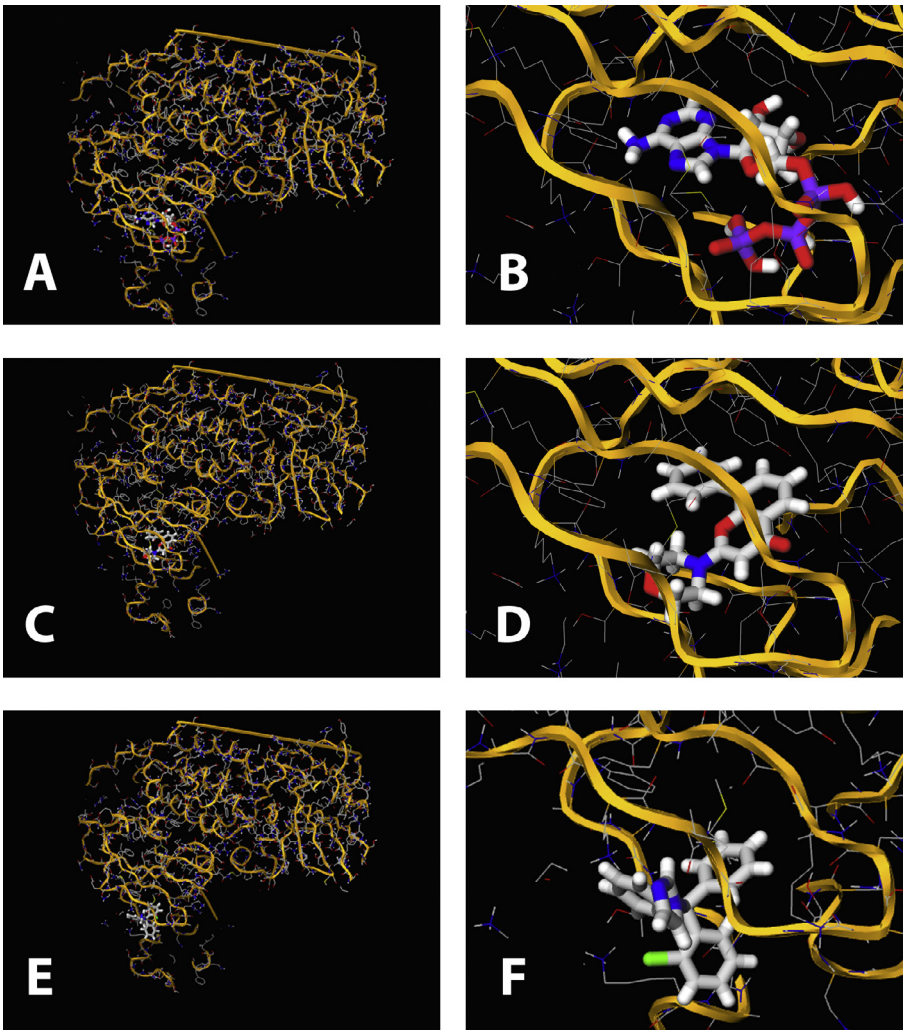

Fig. 6. CTZ docks to ATP binding site at PI3K such as LY294002. Dockings were performed as described in Section 2. Panels (A) and (B): ATP docking for whole enzyme and active site, respectively. Panels (C) and (D): LY294002 docking for whole enzyme and active site, respectively. Panels (E) and (F): CTZ docking for whole enzyme and active site, respectively.

we assessed molecular docking of CTZ on PI3K in which we could observe that CTZ binds to the catalytic shaft of the enzyme, very close to LY294002 and ATP binding sites (Fig. 6). Additionally, the predicted interaction between CTZ and the PI3K catalytic site is relatively strong, presenting a *Z*-score of −6.9, whereas the *Z*-score for ATP and LY294002 are −7.3 and −8.1, respectively. This difference in *Z*-score justifies the highest affinity of the enzyme to LY294002 when compared to both ATP (Walker et al., 2000) and CTZ (Fig. 4J). These results strongly suggest that CTZ directly inhibits PI3K by binding to its catalytic site. Thus, an identical mechanism might be involved on the inhibition of HK, PFK and PK because they are all kinases that have structural similarities in their catalytic sites. It would not be surprising if CTZ inhibits other kinases, such as AMPK, which would partially explain its more potent effects on ATP depletion compared to the other drugs tested herein. In this report, we suggest that PI3K is a putative target for CTZ antitumoral effects, which partly explains the broad effects of the drug.

Acknowledgments

The authors wish to gratefully acknowledge the support of Dr. André Marette (Université Laval, Quebec, QC, Canada) for kindly providing facilities during the sabbatical period of MS-P and PZ. This work was supported by grants from Coordenação de Aperfeiçoamento de Pessoal de Nível Superior (CAPES), Fundação do Câncer/Programa de Oncobiologia-UFRJ, Fundação Carlos Chagas Filho de Amparo à Pesquisa do Estado do Rio de Janeiro (FAPERJ) and Conselho Nacional de Desenvolvimento Científico e Tecnológico (CNPq).

References

Akinleye A, Avvaru P, Furqan M, Song Y, Liu D. Phosphatidylinositol 3-kinase (PI3K) inhibitors as cancer therapeutics. J Hematol Oncol 2013;6:88.
Bayley JP, Devilee P. The Warburg effect in 2012. Curr Opin Oncol 2012;24:62–7.
Beck JT, Ismail A, Tolomeo C. Targeting the phosphatidylinositol 3-kinase (PI3K)/AKT/mammalian target of rapamycin (mTOR) pathway: an emerging treatment strategy for squamous cell lung carcinoma. Cancer Treat Rev 2014;40:980–9.
Brana I, Siu LL. Clinical development of phosphatidylinositol 3-kinase inhibitors for cancer treatment. BMC Med 2012;10:161.
Castillo JJ, Iyengar M, Kuritzky B, Bishop KD. Isotype-specific inhibition of the phosphatidylinositol-3-kinase pathway in hematologic malignancies. Onco Targets Ther 2014;7:333–42.
Coelho RG, Calaca IdC, Celestrini DdM, Correia AH, Costa MA, Sola-Penna M. Clotrimazole disrupts glycolysis in human breast cancer without affecting non-tumoral tissues. Mol Gen Metab 2011;103:394–8.
Furtado CM, Marcondes MC, Sola-Penna M, de Souza MLS, Zancan P. Clotrimazole preferentially inhibits human breast cancer cell proliferation, viability and glycolysis. PLOS ONE 2012;7.
Glass-Marmor L, Beitner R. Detachment of glycolytic enzymes from cytoskeleton of melanoma cells induced by calmodulin antagonists. Eur J Pharmacol 1997;328:241–8.

Glass-Marmor L, Morgenstern H, Beitner R. Calmodulin antagonists decrease glucose 1,6-bisphosphate, fructose 1,6-bisphosphate, ATP and viability of melanoma cells. Eur J Pharmacol 1996;313:265–71.
Gual P, Le Marchand-Brustel Y, Tanti JF. Positive and negative regulation of insulin signaling through IRS-1 phosphorylation. Biochimie 2005;87:99–109.
Hanahan D, Weinberg RA. Hallmarks of cancer: the next generation. Cell 2011;144:646–74.
Hashimoto K, Tsuda H, Koizumi F, Shimizu C, Yonemori K, Ando M, et al. Activated PI3K/AKT and MAPK pathways are potential good prognostic markers in node-positive, triple-negative breast cancer. Ann Oncol 2014;25(10):1973–9.
Khalid MH, Tokunaga Y, Caputy AJ, Walters E. Inhibition of tumor growth and prolonged survival of rats with intracranial gliomas following administration of clotrimazole. J Neurosurg 2005;103:79–86.
Leite TC, Coelho RG, Da Silva D, Coelho WS, Marinho-Carvalho MM, Sola-Penna M. Lactate downregulates the glycolytic enzymes hexokinase and phosphofructokinase in diverse tissues from mice. FEBS Lett 2011;585:92–8.
Lowry OH, Rosebrough NJ, Farr AL, Randall RJ. Protein measurement with the Folin phenol reagent. J Biol Chem 1951;193:265–75.
Majewski N, Nogueira V, Bhaskar P, Coy PE, Skeen JE, Gottlob K, et al. Hexokinase–mitochondria interaction mediated by Akt is required to inhibit apoptosis in the presence or absence of Bax and Bak. Mol Cell 2004;16:819–30.
Marcondes MC, Sola-Penna M, Zancan P. Clotrimazole potentiates the inhibitory effects of ATP on the key glycolytic enzyme 6-phosphofructo-1-kinase. Arch Biochem Biophys 2010;497:62–7.
Meira D, Marinho-Carvalho M, Teixeira C, Veiga V, Da Poian A, Holandino C, et al. Clotrimazole decreases human breast cancer cells viability through alterations in cytoskeleton-associated glycolytic enzymes. Mol Gen Metab 2005;84:354–62.
Mosmann T. Rapid colorimetric assay for cellular growth and survival: application to proliferation and cytotoxicity assays. J Immunol Methods 1983;65:55–63.
O Farrell F, Rusten TE, Stenmark H. Phosphoinositide 3-kinases as accelerators and brakes of autophagy. FEBS J 2013;280:6322–37.
Paplomata E, O'Regan R. The PI3K/AKT/mTOR pathway in breast cancer: targets, trials and biomarkers. Therap Adv Med Oncol 2014;6:154–66.
Parks SK, Chiche J, Pouyssegur J. Disrupting proton dynamics and energy metabolism for cancer therapy. Nat Rev Cancer 2013;13:611–23.
Penso J, Beitner R. Clotrimazole and bifonazole detach hexokinase from mitochondria of melanoma cells. Eur J Pharmacol 1998;342:113–7.
Penso J, Beitner R. Clotrimazole decreases glycolysis and the viability of lung carcinoma and colon adenocarcinoma cells. Eur J Pharmacol 2002a;451:227–35.
Penso J, Beitner R. Detachment of glycolytic enzymes from cytoskeleton of Lewis lung carcinoma and colon adenocarcinoma cells induced by clotrimazole and its correlation to cell viability and morphology. Mol Genet Metab 2002b;76:181–8.
Real-Hohn A, Zancan P, Da Silva D, Martins ER, Salgado LT, Mermelstein CS, et al. Filamentous actin and its associated binding proteins are the stimulatory site for 6-phosphofructo-1-kinase association within the membrane of human erythrocytes. Biochimie 2010;92:538–44.
Rodríguez-Enríquez S, Marín-Hernández A, Gallardo-Pérez JC, Carreño-Fuentes L, Moreno-Sánchez R. Targeting of cancer energy metabolism. Mol Nutr Food Res 2009;53:29–48.
Semenza GL. Targeting HIF-1 for cancer therapy. Nat Rev Cancer 2003;3:721–32.
Semenza GL. Tumor metabolism: cancer cells give and take lactate. J Clin Investig 2008;118:3835–7.
Semenza GL. Hypoxia-inducible factors in physiology and medicine. Cell 2012a;148:399–408.
Semenza GL. Hypoxia-inducible factors: mediators of cancer progression and targets for cancer therapy. Trends Pharmacol Sci 2012b;33:207–14.
Semenza GL. Molecular mechanisms mediating metastasis of hypoxic breast cancer cells. Trends Mol Med 2012c;18:534–43.
Semenza GL. HIF-1 mediates metabolic responses to intratumoral hypoxia and oncogenic mutations. J Clin Investig 2013;123:3664–71.
Spitz GA, Furtado CM, Sola-Penna M, Zancan P. Acetylsalicylic acid and salicylic acid decrease tumor cell viability and glucose metabolism modulating 6-phosphofructo-1-kinase structure and activity. Biochem Pharmacol 2009;77:46–53.
Tallarida RJ. Drug synergism: its detection and applications. J Pharmacol Exp Therap 2001;298:865–72.
Tam J, Cinar R, Liu J, Godlewski G, Wesley D, Jourdan T, et al. Peripheral cannabinoid-1 receptor inverse agonism reduces obesity by reversing leptin resistance. Cell Metab 2012;16:167–79.
Tremblay F, Marette A. Amino acid and insulin signaling via the mTOR/p70 S6 kinase pathway. A negative feedback mechanism leading to insulin resistance in skeletal muscle cells. J Biol Chem 2001;276:38052–60.
Voskas D, Ling LS, Woodgett JR. Signals controlling un-differentiated states in embryonic stem and cancer cells: role of the phosphatidylinositol 3′ kinase pathway. J Cell Physiol 2014;229:1312–22.
Walker EH, Pacold ME, Perisic O, Stephens L, Hawkins PT, Wymann MP, et al. Structural determinants of phosphoinositide 3-kinase inhibition by wortmannin, LY294002, quercetin, myricetin, and staurosporine. Mol Cell 2000;6:909–19.
Wong CC, Zhang H, Gilkes DM, Chen J, Wei H, Chaturvedi P, et al. Inhibitors of hypoxia-inducible factor 1 block breast cancer metastatic niche formation and lung metastasis. J Mol Med (Berl) 2012;90(7):803–15.
Xu Y, Li N, Xiang R, Sun P. Emerging roles of the p38 MAPK and PI3K/AKT/mTOR pathways in oncogene-induced senescence. Trends Biochem Sci 2014;39:268–76.
Yeung S, Pan J, Lee MH. Roles of p53, Myc and HIF-1 in regulating glycolysis – the seventh hallmark of cancer. Cell Mol Life Sci 2008;65:3981–99.
Zancan P, Rosas AO, Marcondes MC, Marinho-Carvalho MM, Sola-Penna M. Clotrimazole inhibits and modulates heterologous association of the key glycolytic enzyme 6-phosphofructo-1-kinase. Biochem Pharmacol 2007;73:1520–7.
Zancan P, Sola-Penna M, Furtado CM, Da Silva D. Differential expression of phosphofructokinase-1 isoforms correlates with the glycolytic efficiency of breast cancer cells. Mol Gen Metab 2010;100:372–8.
Zheng J. Energy metabolism of cancer: glycolysis versus oxidative phosphorylation (review). Oncol Lett 2012;4:1151–7.
Zu XL, Guppy M. Cancer metabolism: facts, fantasy, and fiction. Biochem Biophys Res Commun 2004;313:459–65.